

Inhibition of Sphingomyelin Synthesis Reduces Atherogenesis in Apolipoprotein E-Knockout Mice

Tae-Sik Park, PhD; Robert L. Panek, PhD; Sandra Bak Mueller, MS; Jeffrey C. Hanselman, BS; Wendy S. Rosebury, HT (ASCP); Andrew W. Robertson, HT (ASCP); Erick K. Kindt, BS, MBA; Reynold Homan, PhD; Sotirios K. Karathanasis, PhD; Mark D. Reikter, MD, PhD

Background—In clinical studies, sphingomyelin (SM) plasma levels correlated with the occurrence of coronary heart disease independently of plasma cholesterol levels. We hypothesized that inhibition of SM synthesis would have antiatherogenic effects. To test this hypothesis, apolipoprotein E (apoE)–knockout (KO) mice were treated with myriocin, a potent inhibitor of serine palmitoyltransferase, the rate-limiting enzyme in SM biosynthesis.

Methods and Results—Diet-admix treatment of apoE-KO mice with myriocin in Western diet for 12 weeks lowered SM and sphinganine plasma levels. Decreases in sphinganine and SM concentrations were also observed in the liver and aorta of myriocin-treated animals compared with controls. Inhibition of de novo sphingolipid biosynthesis reduced total cholesterol and triglyceride plasma levels. Cholesterol distribution in lipoproteins demonstrated a decrease in β -VLDL and LDL cholesterol and an increase in HDL cholesterol. Oil red O staining of total aortas demonstrated reduction of atherosclerotic lesion coverage in the myriocin-treated group. Atherosclerotic plaque area was also reduced in the aortic root and brachiocephalic artery.

Conclusions—Inhibition of de novo SM biosynthesis in apoE-KO mice lowers plasma cholesterol and triglyceride levels, raises HDL cholesterol, and prevents development of atherosclerotic lesions. (*Circulation*. 2004;110:3465-3471.)

Key Words: sphingomyelin ■ inhibitors ■ cholesterol ■ lipoproteins ■ atherosclerosis

Sphingomyelin (SM) is one of the major lipids in plasma lipoproteins and cell membranes. In clinical studies, SM plasma levels correlated with the occurrence of coronary heart disease independently of plasma cholesterol levels.¹ SM and its derivatives are accumulated in human and experimental atherosclerotic lesions.²

See p 3400

Although direct mechanistic links between SM and atherosclerosis have not been established, available in vitro data suggest that SM might have the following proatherogenic properties. First, SM content of lipoprotein particles may influence lipid metabolism by affecting binding or activity of lecithin-cholesterol acyltransferase³ and lipoprotein lipase.⁴ Second, SM-rich lipoproteins can be converted to foam cell substrates by sphingomyelinase (SMase) in the artery wall,⁵ thereby promoting foam cell formation. Third, ceramide and related products of SM synthesis and breakdown are potent regulators of cell proliferation, activation, and apoptosis⁶ and hence may affect plaque growth and stability. Thus, inhibition of SM synthesis may have antiatherogenic effects.

Serine palmitoyltransferase (SPT) catalyzes the first committed step in sphingolipid synthesis. SPT condenses the palmitic acid of palmitoyl-coenzyme A with serine to produce ketosph-

inganine, the precursor to the unique aminolipid backbone that is characteristic of all sphingolipids.⁷ SPT is composed of 2 different subunits, LCB1 and LCB2.⁸ Myriocin is a potent and specific SPT inhibitor isolated from fungi⁹ and in high doses is known to have a potent immunosuppressive activity.¹⁰

In current studies, we investigated the effect of SM biosynthesis on plasma cholesterol and triglycerides (TGs). We have demonstrated that myriocin, a potent SPT inhibitor, improved the lipid profiles and reduced atherogenesis in apolipoprotein E (apoE)–knockout (KO) mice.

Methods

Animal Experiments

Male C57Bl/6J and apoE-KO mice on C57Bl/6J background were obtained from the Jackson Laboratory (Bar Harbor, Me). Myriocin was mixed with Western diet containing 0.21% cholesterol and 21% fat. Eight- to 12-week-old apoE-KO (n=16) mice received myriocin 0.3 mg · kg⁻¹ · d⁻¹ for 12 weeks. A myriocin dose was chosen from a previous dose-dependent experiment with apoE-KO mice (M.D.R., unpublished data, 2002). Control groups consisted of apoE-KO mice fed standard chow or Western diet without myriocin and standard chow-fed C57Bl/6J mice (n=16). Body weight and chow feeding were measured every week to examine the food consumption. All procedures and protocols involving the use of animals were approved by the Pfizer Animal Care and Use Committee and conformed with the “Guide for the Care and Use of Laboratory Animals” published

Received April 28, 2004; revision received September 21, 2004; accepted September 30, 2004.

From Cardiovascular Pharmacology, Pfizer Global Research and Development, Ann Arbor, Mich.

Correspondence to Dr Robert L. Panek, Cardiovascular Pharmacology, Pfizer Global Research and Development, 2800 Plymouth Rd, Ann Arbor, MI 48105. E-mail robert.panek@pfizer.com

© 2004 American Heart Association, Inc.

Circulation is available at <http://www.circulationaha.org>

DOI: 10.1161/01.CIR.0000148370.60535.22

by the US National Institutes of Health (NIH publication No. 85-23, revised 1996).

SPT Expression and Activity

Total RNA was isolated from liver and aorta with TriZol (Invitrogen). LCB1 and LCB2 mRNA levels were measured by real-time polymerase chain reaction on ABI Prism 7900HT Sequence Detection System (Applied Biosystems). The following primers and probe sets were used: LCB1, forward primer 5'-CCGCTCCTTC-GTGGTTGA-3', reverse primer 5'-GAGGTAACGAAAGCAGAA-AAGCAG-3', probe 5'⁶FAM-TCAGCGGCTCTCCGGTCAA-GGAT-TAMRA3'; LCB2, forward primer 5'-CTGGATG-AGGCTCACAGCATT-3', reverse primer 5'-CCTCAGGAT-CCAGGCCAA-3', probe, 5'⁶FAM- CCTCAGGGCGAGGCG-TGGTAGAT-TAMRA3'. The optimum number of cycles was set for each gene product with uniform amplification. Each mRNA level was expressed as a ratio to GAPDH RNA. Liver tissues from each group were homogenized, and SPT activity was measured with ¹⁴C-serine and palmitoyl-coenzyme A as substrates and thin-layer chromatography analysis as described previously.¹¹

Analysis of Sphingolipids and Phospholipids by LC/MS/MS and High-Performance Liquid Chromatography

Total lipids were extracted by the modified method of Bligh-Dyer extraction¹² as described previously.¹³ A Micromass (Manchester, United Kingdom) Quattro II tandem quadrupole mass spectrometer with a standard Z-spray ion source, set to electrospray positive ionization mode, with MassLynx version 3.4 operating software, was used for all quantitative determinations. Precursor-to-product ion transitions were established through direct infusion of each compound into the mass spectrometer. The following ion transitions were used for quantification: SM (704→184 m/z), sphinganine (302→284 m/z), ceramide (566→264 m/z), and psychosine (462→282 m/z) as an internal standard. For our instrument, at a collision cell pressure of 2×10^{-3} mbar of argon, cone and collision voltages were as follows: SM 40 V and 25 eV, sphinganine 40 V and 15 eV, ceramide 45 V and 25 eV, and psychosine 35 V and 25 eV. A sample volume of 2 μ L was injected into the LC/MS/MS system. Final chromatographic retention times for SM, sphinganine, and psychosine (internal standard) were 1.40, 1.43, and 1.25 minutes, respectively. Lipid extracts were analyzed by high-performance liquid chromatography to determine plasma phosphatidylcholine (PC) levels as described previously.¹⁴

Plasma Lipids

Mice were euthanized by CO₂ inhalation, and blood was collected through cardiac puncture. Plasma concentrations of total cholesterol and triglyceride were determined enzymatically on a Cobas Mira Plus autoanalyzer with the cholesterol R1 and triglycerides reagent methods, respectively (Roche Diagnostics). Colorimetric changes were measured at 500 nm. Lipoproteins were separated from mouse plasma by fast-protein liquid chromatography with a Superose 6HR column. Cholesterol distribution among lipoproteins was determined by in-line post column analysis as described previously.¹⁵

Vascular Pathology

For quantitative analysis of atherosclerotic lesion coverage, euthanized mice were perfused with saline, and the aorta was isolated from the heart to the iliac bifurcation by severing of the minor branching arteries and dissection of the adventitia. After 24 hours of fixation with 10% buffered formalin, the aorta was opened longitudinally and pinned down on black wax. Lipids were stained with oil red O, and photographs were taken. The percentage of aorta stained with oil red O was determined by image analysis software (Image Pro Plus).

For histological analysis, the mice were perfused and fixed in zinc-Tris fixative. Paraffin-embedded sections were stained with Masson's trichrome. Macrophages were immunohistochemically stained with MAC-2 antibody (clone M3/38 from Cedar lane

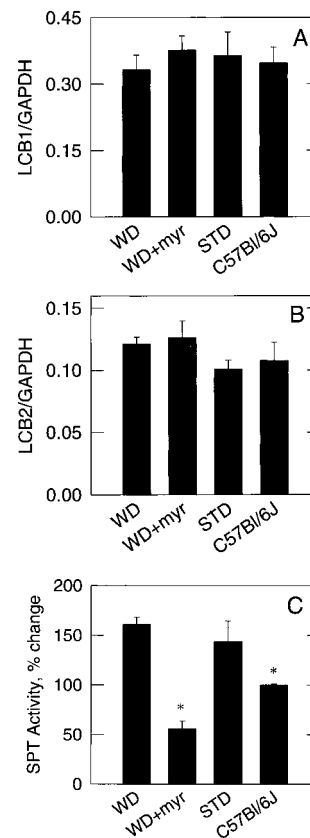


Figure 1. SPT gene expression and enzyme activity. mRNA and cell-free homogenate were prepared from liver. SPT mRNA expression was quantified by quantitative real-time polymerase chain reaction. Expression was described as ratio of LCB1 (A) or LCB2 (B) mRNA to rodent GAPDH RNA ($n=5$, $P>0.05$). SPT activity of cell-free homogenate (C) was measured with ¹⁴C-labeled serine and palmitoyl-coenzyme A as substrates and analyzed by thin-layer chromatography. Relative amounts of 3-ketosphinganine were determined by densitometry scanning. Values are mean \pm SEM ($n=3$, * $P<0.05$). WD indicates Western diet chow; WD+myr, Western diet chow plus myriocin; and STD, standard chow.

Laboratories Limited) counterstained with Verhoeff elastic stain. T lymphocytes were immunohistochemically stained with rat CD3 antibody (clone CD3-12, Serotec). Lesion thickness and area occupied by macrophages were determined with Image Pro Plus software.

Statistical Analysis

Results are expressed as mean \pm SEM. Comparisons among several groups were determined by 1-way ANOVA with Dunnett's post hoc analysis using PRISM 2.01. If a significant difference was found among groups, distribution-free multiple comparisons were performed to find significance among groups. When SEMs were unequal, a nonparametric test (Mann-Whitney) was used to calculate the level of significance. Results were considered significant at $P<0.05$.

Results

SPT Gene Expression and Enzyme Activity

Real-time polymerase chain reaction analysis demonstrated that myriocin had no effect on expression of LCB1 and LCB2 mRNA (Figures 1A and 1B). Compared with C57Bl/6J mice, SPT activity was increased in apoE-KO mice fed a Western diet and standard chow, by 60% ($n=3$, $P<0.05$) and

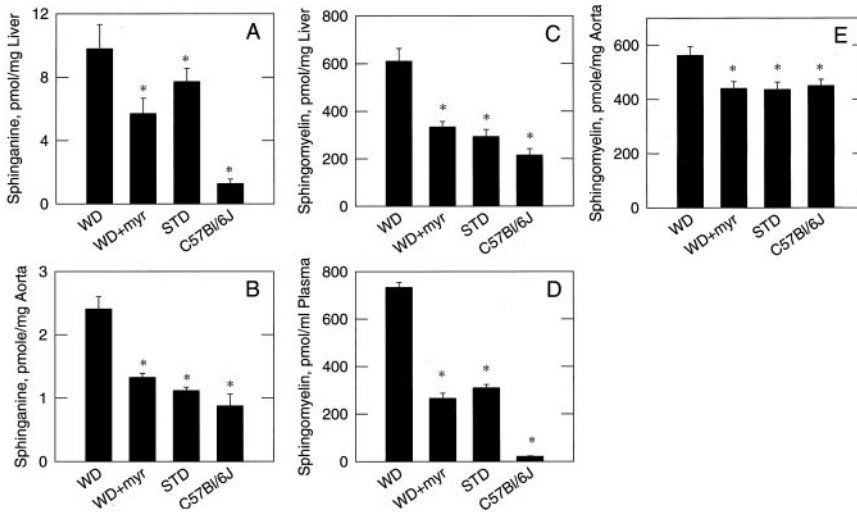


Figure 2. Sphinganine and sphingomyelin concentrations in liver, plasma, and aorta. After 12 weeks of myriocin treatment, mice were euthanized, and plasma, liver, and aorta were isolated. Total lipids were extracted by Blier-Dyer method. Sphinganine levels in liver (A) and aorta (B) and SM levels in liver (C), plasma (D), and aorta (E) were determined by LC/MS as described in Methods. Values are mean \pm SEM ($n=5$, $*P<0.05$). WD indicates Western diet chow; WD+myr, Western diet chow plus myriocin; and STD, standard chow.

43% ($n=3$, $P<0.05$), respectively (Figure 1C). Myriocin dramatically lowered SPT activity in the Western diet-fed apoE-KO mice (66% decrease compared with the untreated Western diet-fed apoE-KO mice and 48% decrease compared with C57Bl/6J control group [$n=3$, $P<0.05$]). Thus, myriocin treatment had no effect on SPT expression but was extremely effective in lowering SPT enzyme activity.

SM Synthesis, Accumulation, and Characteristics

To determine whether inhibition of SPT activity was translated into inhibition of de novo SM production, we measured the quantity of sphinganine, a close downstream marker of SPT activity that cannot be influenced by SM degradation via SMase. Sphinganine levels were significantly increased in Western diet-fed and chow-fed apoE-KO mice compared with control C57Bl/6J mice, which indicates an increased rate of SM synthesis in this model of atherosclerosis. Myriocin treatment lowered sphinganine levels in liver by 42% compared with the Western diet-fed group (Figure 2A).

In aorta, sphinganine levels in the myriocin-treated apoE-KO group, standard chow-fed apoE-KO group, and C57Bl/6J group were decreased by 45%, 54%, and 63%, respectively, compared with the Western diet-fed group (Figure 2B). Sphinganine in plasma was below detectable levels. Thus, myriocin treatment inhibited the SM synthetic pathway in both liver and aorta.

Although SM levels are determined by both synthesis and degradation, in the present experimental system, SM changes were generally associated with changes in SPT activity and sphinganine production, which emphasizes the role of the SPT-dependent synthetic pathway. Specifically, SM levels in the liver of C57Bl/6J mice were 65% lower than those in Western diet-fed apoE-KO mice (myriocin-treated and standard chow-fed alike). Myriocin treatment lowered SM accumulation in the liver by 45% compared with Western diet-fed apoE-KO mice (Figure 2C). Moreover, Western diet-fed apoE-KO mice displayed the highest level of plasma SM, 33 times higher than C57Bl/6J and >2 times higher than the standard chow-fed apoE-KO mice (Figure 2D). Myriocin treatment lowered plasma SM in Western diet-fed apoE-KO mice by 64%, bringing it to the level of their standard

chow-fed counterparts. Small differences were observed among aortas after the various treatments; however, there were statistically significant differences between Western diet-fed apoE-KO and control mice. Myriocin decreased SM levels by 20% (Figure 2E). Thus, SPT inhibition by myriocin drastically affected SM production and accumulation.

Certain SM features may determine its fate and potential role in atherosclerosis. Secretory SMase is known to cause SM hydrolysis to generate ceramide, which stimulates aggregation of lipoproteins and foam cell formation.⁵ The high SM/PC ratio in lipoproteins determines their susceptibility to SMase. We measured the plasma SM/PC ratio using high-performance liquid chromatography. Although plasma SM and PC levels were substantially lower in the myriocin-treated group than in the Western diet-fed group, myriocin did not affect the plasma SM/PC ratio (Figure 3A). On the other hand, myriocin treatment reduced ceramide levels by 60%, which is comparable to the standard chow-fed group (Figure 3B). The lowest ceramide levels were found in the C57Bl/6J control group. Thus, the myriocin-induced reduction of SM accumulation was accompanied by a substantial reduction in ceramide levels and was not associated with any changes in the SM/PC ratio.

Plasma Cholesterol and TGs

Because the SM content of lipoproteins affects the activities of enzymes involved in lipid metabolism *in vitro*,^{3,4} we questioned whether the inhibition of sphingolipid biosynthesis affected cholesterol and TG levels in plasma. As expected, plasma cholesterol and TGs were highest in the Western diet-fed apoE-KO mice and lowest in C57Bl/6J mice, with standard chow-fed apoE-KO mice positioned in between. Myriocin exhibited significant lipid-lowering activity by bringing both parameters to the levels of standard chow-fed apoE-KO mice. Myriocin lowered plasma cholesterol and TGs by 41% and 45%, respectively (Figure 4). In addition, myriocin lowered β -VLDL and LDL cholesterol levels by 51% and 35%, respectively. In contrast, HDL cholesterol content was increased by 54% (Figure 5). Cholesterol distribution in lipoproteins of standard chow-fed apoE-KO mice was comparable to that in myriocin-treated mice. Compared

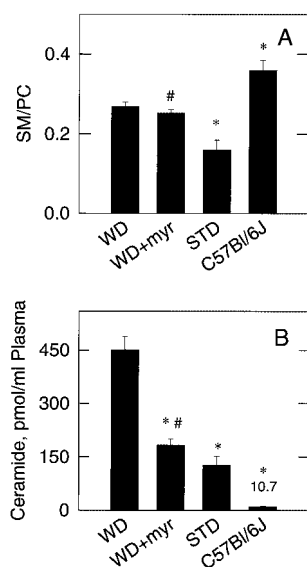


Figure 3. SM/PC ratio and ceramide concentrations in plasma. Plasma concentrations of SM and PC were determined as described in Methods, and SM/PC ratio (A) was calculated. Plasma ceramide levels (B) were analyzed by LC/MS/MS. Values are mean \pm SEM (n=5; * P <0.01, Western diet vs Western diet plus myriocin; # P <0.05, standard chow vs Western diet plus myriocin). WD indicates Western diet chow; WD+myr; Western diet chow plus myriocin; and STD, standard chow.

with apoE-KO mice, the WT C57Bl/6J mice showed very low total cholesterol in plasma. Most of the cholesterol content in C57Bl/6J was found in HDL. In addition, myriocin lowered plasma apoB levels, which were comparable to those in the standard chow-fed group (T.-S. Park, unpublished data, 2004). Because plasma apoB levels, especially apoB100 levels, in LDL correlate with atherogenesis,¹⁶ the apoB-lowering effect might contribute to prevention of atherogen-

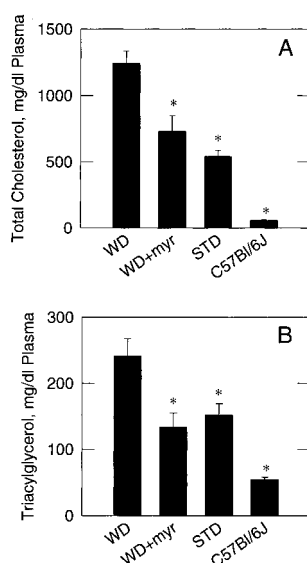


Figure 4. Cholesterol and TG concentrations in plasma. Plasma concentrations of total cholesterol (A) and TG (B) were determined as described in Methods. Values are mean \pm SEM (n=5, * P <0.01). WD indicates Western diet chow; WD+myr; Western diet chow plus myriocin; and STD, standard chow.

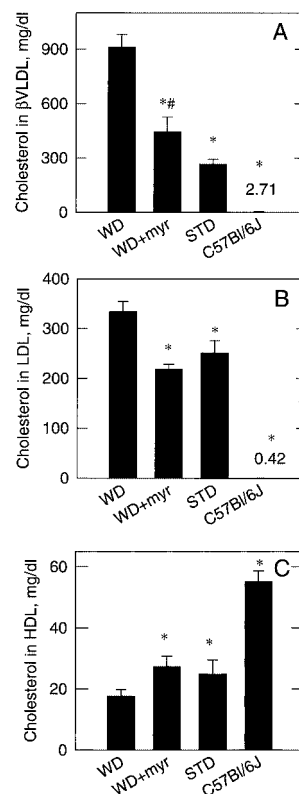


Figure 5. Cholesterol distribution in lipoproteins. Plasma lipoproteins were separated by fast protein liquid chromatography, and cholesterol contents in β -VLDL (A), LDL (B), and HDL (C) were determined as described in Methods. Values are mean \pm SEM (n=5, * P <0.01, Western diet vs other study groups; n=5, # P <0.05, Western diet plus myriocin vs standard chow). WD indicates Western diet chow; WD+myr; Western diet chow plus myriocin; and STD, standard chow.

esis by myriocin. Thus, myriocin exerted profound lipid-lowering effects.

Atherogenesis

Oil red O staining of en face aortas revealed that myriocin treatment reduced atherosclerotic lesion coverage in Western diet-fed apoE-KO mice by 93% (Figure 6). Growth of atherosclerotic lesions in the brachiocephalic artery and aortic valve area was also significantly inhibited (Figure 7). In the brachiocephalic artery, myriocin treatment led to a 76% decrease in lesion area and a 74% decrease in macrophage area. Lesions in myriocin-treated, Western diet-fed apoE-KO mice did not develop a necrotic core. In the aortic root, lesion area was decreased by 44% and macrophage area was decreased by 31% with myriocin treatment. Accumulation of T cells was not affected by myriocin treatment (Figure 8). Thus, SPT inhibition had substantial antiatherogenic effects.

Discussion

We have demonstrated that SM content and production were proportionally increased in plasma, liver, and aorta of the Western diet-fed apoE-KO mice compared with standard chow-fed apoE-KO and C57Bl/6J control mice. Myriocin, a specific inhibitor of SPT, inhibited de novo SM synthesis in the liver and aorta, and this was associated with reductions of

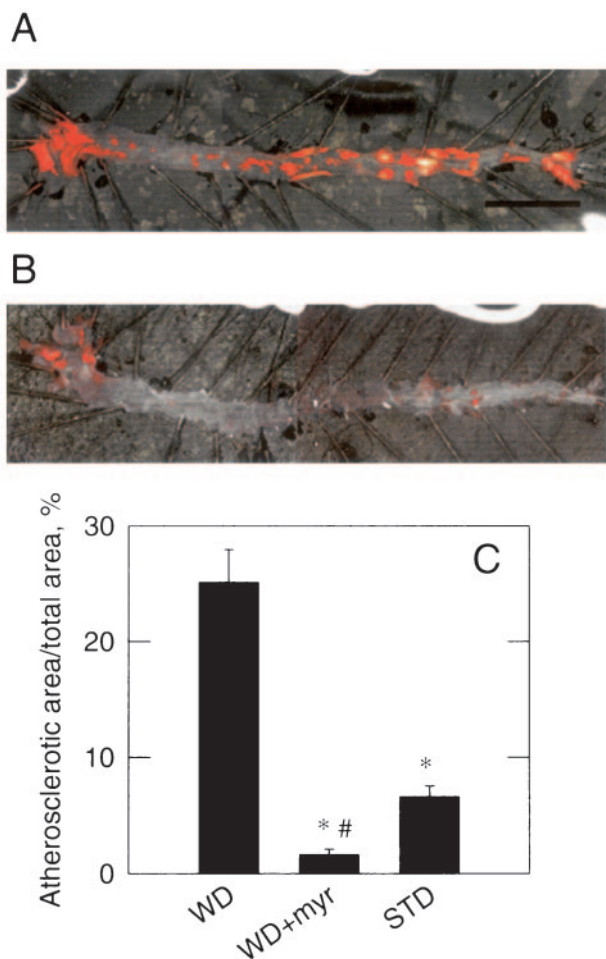


Figure 6. Lipid deposition in aortas of Western diet-fed apoE-KO mice. ApoE-KO mice were fed with Western diet in presence (A) or absence (B) of myriocin for 12 weeks. Mice were euthanized and fixed with 10% buffered formalin for 24 hours. Aorta from heart to iliac bifurcation was dissected, opened along ventral surface, and pinned down on black wax background. Accumulated lipids were visualized by oil red O staining. Areas of atherosclerotic lesion were quantified by Image Pro Plus (C) and represented as percentage of lesion area to total aorta area. Values are mean±SEM (n=4; *P<0.01, Western diet vs Western diet plus myriocin or standard chow; #P<0.01, standard chow vs Western diet plus myriocin). Bar represents 1 cm. WD indicates Western diet chow; WD+myr; Western diet chow plus myriocin; and STD, standard chow.

plasma SM and ceramide that were not accompanied by changes in the SM/PC ratio. Inhibition of SM synthesis led to the lowering of plasma cholesterol and TGs. These changes were associated with dramatic antiatherosclerotic effects.

Increased plasma SM levels previously have been linked to enhanced SPT activity in the liver of apoE-KO mice.¹⁷ The present data support this observation and provide further evidence that SPT inhibition by myriocin leads to a reduction of plasma SM. Plasma SM is a component of lipoprotein particles and has been suggested to be proatherogenic.^{1,18} Intermediates of SM synthesis, in particular ceramide, also possess independent proatherogenic properties. Ceramide plays an important role in lipoprotein aggregation and may promote foam cell formation.¹⁸ It is a potent regulator of cell proliferation, activation, and apoptosis⁶ and hence may affect

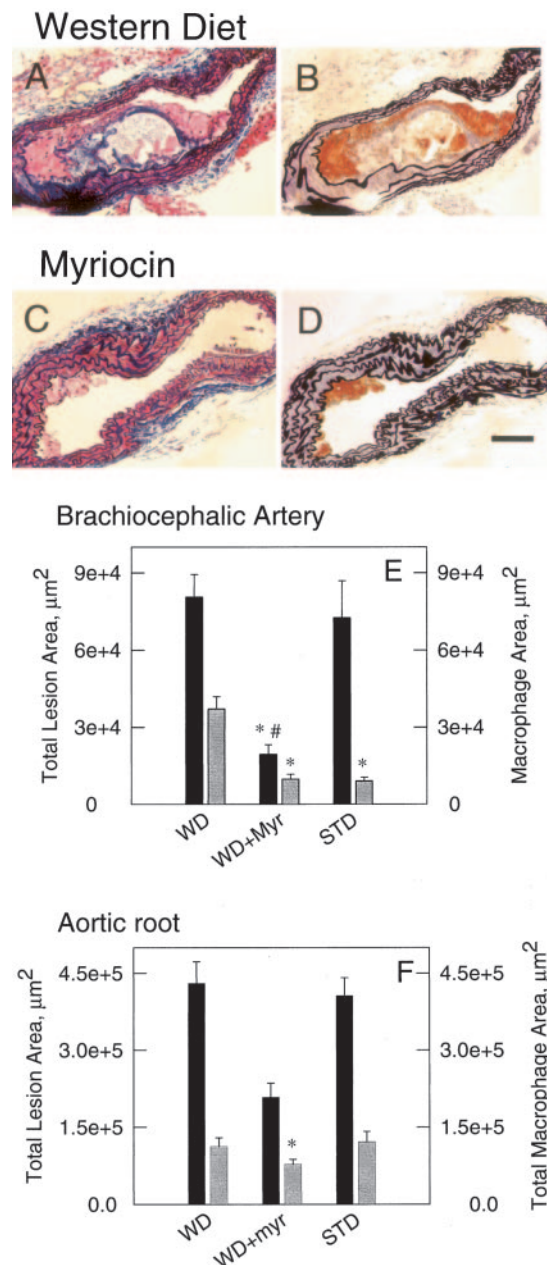


Figure 7. Formation of atherosclerotic lesions in brachiocephalic artery and aortic root. Cross section of brachiocephalic artery was stained by Masson's trichrome (A, C) and MAC-2 antibody counterstained with Verhoeff elastic stain (B, D). Atherosclerotic lesion (black bars) and macrophage size (gray bars) in brachiocephalic artery (E) and in aortic root (F) were quantified by Image Pro Plus (E). Values are mean±SEM (n=5; *P<0.01, Western diet vs Western diet plus myriocin; #P<0.01, standard chow vs Western diet plus myriocin). Bar represents 100 μm. WD indicates Western diet chow; WD+myr; Western diet chow plus myriocin; and STD, standard chow.

plaque growth and stability. We demonstrated the ceramide-lowering effects of myriocin. It is not absolutely certain that these effects are driven by inhibition of ceramide production. An alternative source of ceramide is SM hydrolysis by SMase; however, the present data suggest that the synthetic arm of the pathway is more likely to be affected by myriocin. At physiological pH, recombinant human secretory SMase

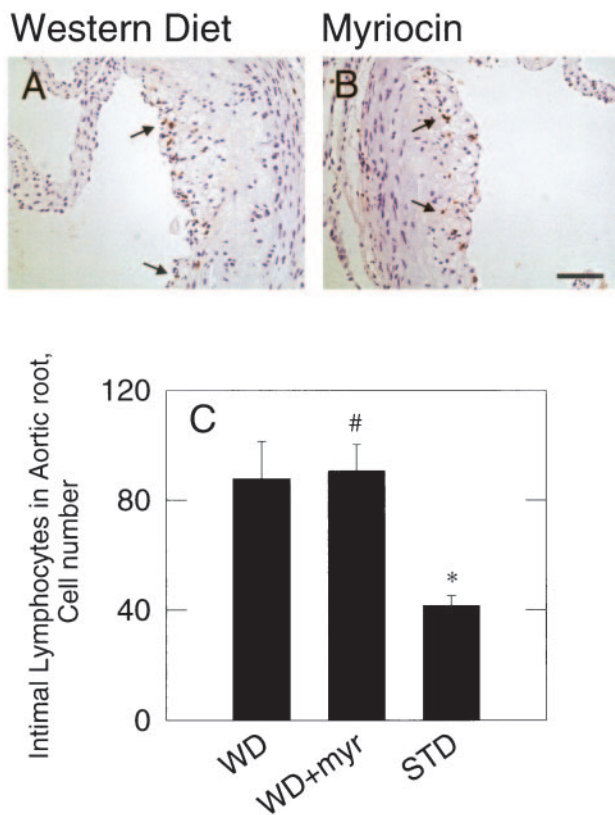


Figure 8. Incorporation of T lymphocytes into lesion of aortic root. Cross section of aortic root was stained by rat CD3 antibody and developed by diaminobenzidine (brown color) to detect incorporated T lymphocytes (A, B). Sections were counterstained with Harris hematoxylin (blue). T-lymphocyte incorporation was quantified by measuring number of intimal T lymphocytes in aortic root (C). Values are mean \pm SEM (n=5; * P <0.05, Western diet vs standard chow; # P <0.05, Western diet plus myriocin vs standard chow). Bar represents 50 μ m. WD indicates Western diet chow; WD+myr; Western diet chow plus myriocin; and STD, standard chow.

preferentially acts on lipoproteins with a high SM/PC ratio⁵; however, we found no difference in SM/PC ratio between the Western diet-fed and myriocin-treated groups. Thus, myriocin is likely to inhibit ceramide synthesis, which in turn can be partially responsible for the antiatherogenic activity of this compound.

SM has been shown to negatively affect the rate of lipoprotein lipase-mediated lipolysis in lipid emulsions.⁴ Extrapolation of this phenomenon to the *in vivo* situation is suggestive of accelerated lipolysis associated with SM depletion. This mechanism could be involved in the TG lowering that we observed in myriocin-treated mice. The precise mechanism for total cholesterol lowering in myriocin-treated mice is unclear. We suggest that lipid lowering may be driven by SM-dependent inhibition of cholesterol synthesis, at least in part. SM, a major plasma membrane component, has a high affinity for free cholesterol.¹⁹ It is conceivable that inhibition of SM synthesis leads to a reduced SM concentration in the plasma membrane of hepatocytes, thereby inducing release of free cholesterol into the cytoplasm. Increased intracellular concentrations of free cholesterol could be sensed as a signal to inhibit cholesterol synthesis. Recent findings demonstrated that

inhibition of sphingolipid biosynthesis caused suppression of lipogenic gene expression in Chinese hamster ovary cells.²⁰ This hypothesis, however, needs further *in vivo* testing.

SM depletion was also associated with an elevation of HDL. *In vitro* data suggest that increased SM content in lipoproteins can inhibit key enzymes involved in lipoprotein metabolism.^{3,4} It has also been demonstrated that SM in macrophage membranes interfered with reverse cholesterol transport.²¹ It is conceivable that SM depletion would lead to activation of reverse cholesterol transport and contribute to elevation of HDL cholesterol, which is consistent with observations from the present study; however, further studies are needed to explore effects of SM depletion on reverse cholesterol transport and, ultimately, atherogenesis.

We have demonstrated that inhibition of SM synthesis was associated with a significant reduction in atherosclerotic lesion formation in apoE-KO mice. Because plaque formation in apoE-KO mice is lipid-driven,²² the observed antiatherogenic effects were likely indirect, due to normalization of plasma lipids as a result of the inhibition of SM synthesis by liver; however, we have also shown local inhibition of SM production in aorta. Myriocin-treated, Western diet-fed apoE-KO mice showed a plasma lipid profile similar to that in the standard chow-fed apoE-KO mice, but their lesions were significantly smaller. Taken together, these findings suggest that the antiatherogenic effects of myriocin could be attributed in part to local inhibition of SPT in the arterial wall.

Myriocin may potentially influence atherogenesis in an SPT-independent manner, eg, by inhibition of lipid absorption from the gut or by exertion of its immunomodulatory properties.^{9,10} The potential role of myriocin or sphingolipids on lipid absorption has not been examined, and additional studies are warranted. Nonspecific immunomodulatory effects of myriocin also cannot be ruled out completely.

Indeed, a myriocin analogue (FTY720) devoid of SPT activity is a potent immunosuppressor.²³ The predominant mechanism of action of FTY720 is immunosuppression via sphingosine-1-phosphate (S1P) receptor agonism.²³ However, we suggest that S1P agonism does not play a leading role in the observed atheroprotective phenomena for the following reasons. First, to the best of our knowledge, there are no published data suggesting an influence of S1P on plasma SM and lipoproteins. To the contrary, SM- and lipid-lowering effects were correlated with inhibition of SM synthesis, as shown by significant lowering of sphinganine concentrations. Second, S1P agonism has diverse effects on various aspects of atherosclerosis, but an overall proatherogenic and prothrombotic activity is suggested.²⁴ Specifically, it activates macrophages.²⁵ In contrast, the present data demonstrate a significant decrease in both total plaque and macrophage area. Third, immunosuppressive activity of FTY720 is driven by alteration of lymphocyte trafficking.²³ Although we did not count peripheral blood lymphocytes in the present study, we performed immunostaining of arterial sections with CD3, a T-cell-specific antibody. We have demonstrated that CD3-positive cell staining in this model of atherosclerosis was minimal and was not affected by myriocin. These data, together with the generally accepted fact that atherosclerotic lesion development in apoE-KO mice is

lipid driven,²² indicate that dramatic lipid-lowering effects of myriocin are likely to be responsible for its antiatherogenic activity. It is also likely that direct inhibition of SPT in the vascular wall may be responsible for some additional effects, whereas SPT-independent mechanisms play a minor role.

Although inhibition of SM synthesis may be beneficial for treatment of atherosclerosis, it is still unknown whether the targeting of SPT would be associated with any toxicological issues. LCB1 and LCB2 genes are essential for cell survival, and the changes in SPT activity result in a defective development of the fruit fly and filamentous fungi,^{26,27} as well as hereditary sensory neuropathy type I in humans.^{28,29} In the present study, however, no overt toxicity was associated with chronic administration of myriocin.

In conclusion, SPT inhibition by myriocin in apoE-KO mice effectively inhibited SM synthesis, an effect that was associated with an improved plasma lipid profile and significant antiatherogenic activity. Consistent with these observations are clinical reports indicating that SM is an independent risk factor for coronary heart disease and a plasma marker of coronary artery disease.¹ These data suggest that SPT and potentially other key enzymes regulating SM synthesis could represent a novel class of molecular targets for treatment of dyslipidemia and atherosclerosis.

Acknowledgments

We gratefully acknowledge Dr Mark Kowala and Dr Robert Leadley for helpful discussion and critical reading of the manuscript.

References

- Jiang XC, Paultre F, Pearson TA, Reed RG, Francis CK, Lin M, Berglund L, Tall AR. Plasma sphingomyelin level as a risk factor for coronary artery disease. *Arterioscler Thromb Vasc Biol.* 2000;20:2614–2618.
- Schissel SL, Tweedie-Hardman J, Rapp JH, Graham G, Williams KJ, Tabas I. Rabbit aorta and human atherosclerotic lesions hydrolyze the sphingomyelin of retained low-density lipoprotein: proposed role for arterial-wall sphingomyelinase in subendothelial retention and aggregation of atherogenic lipoproteins. *J Clin Invest.* 1996;98:1455–1464.
- Bolin DJ, Jonas A. Sphingomyelin inhibits the lecithin-cholesterol acyltransferase reaction with reconstituted high density lipoproteins by decreasing enzyme binding. *J Biol Chem.* 1996;271:19152–19158.
- Arimoto I, Saito H, Kawashima Y, Miyajima K, Handa T. Effects of sphingomyelin and cholesterol on lipoprotein lipase-mediated lipolysis in lipid emulsions. *J Lipid Res.* 1998;39:143–151.
- Schissel SL, Jiang X, Tweedie-Hardman J, Jeong T, Camejo EH, Najib J, Rapp JH, Williams KJ, Tabas I. Secretory sphingomyelinase, a product of the acid sphingomyelinase gene, can hydrolyze atherogenic lipoproteins at neutral pH: implications for atherosclerotic lesion development. *J Biol Chem.* 1998;273:2738–2746.
- Maceyka M, Payne SG, Milstien S, Spiegel S. Sphingosine kinase, sphingosine-1-phosphate, and apoptosis. *Biochim Biophys Acta.* 2002;1585:193–201.
- Hanada K, Hara T, Nishijima M, Kuge O, Dickson RC, Nagiec MM. A mammalian homolog of the yeast LCB1 encodes a component of serine palmitoyltransferase, the enzyme catalyzing the first step in sphingolipid synthesis. *J Biol Chem.* 1997;272:32108–32114.
- Weiss B, Stoffel W. Human and murine serine-palmitoyl-CoA transferase: cloning, expression and characterization of the key enzyme in sphingolipid synthesis. *Eur J Biochem.* 1997;249:239–247.
- Miyake Y, Kozutsumi Y, Nakamura S, Fujita T, Kawasaki T. Serine palmitoyltransferase is the primary target of a sphingosine-like immunosuppressant, ISP-1/myriocin. *Biochem Biophys Res Commun.* 1995;211:396–403.
- Fujita T, Inoue K, Yamamoto S, Ikumoto T, Sasaki S, Toyama R, Chiba K, Hoshino Y, Okumoto T. Fungal metabolites, part 11: a potent immunosuppressive activity found in *Isaria sinclairii* metabolite. *J Antibiot (Tokyo).* 1994;47:208–215.
- Gable K, Slife H, Bacikova D, Monaghan E, Dunn TM. Tsc3p is an 80-amino acid protein associated with serine palmitoyltransferase and required for optimal enzyme activity. *J Biol Chem.* 2000;275:7597–7603.
- Bligh EG, Dyer WJ. A rapid method of total lipid extraction and purification. *Can J Med Sci.* 1959;37:911–917.
- Perry DK, Bielawska A, Hannun YA. Quantitative determination of ceramide using diglyceride kinase. *Methods Enzymol.* 2000;312:22–31.
- Homan R, Anderson MK. Rapid separation and quantitation of combined neutral and polar lipid classes by high-performance liquid chromatography and evaporative light-scattering mass detection. *J Chromatogr B Biomed Sci Appl.* 1998;708:21–26.
- Kieft KA, Bocan TM, Krause BR. Rapid on-line determination of cholesterol distribution among plasma lipoproteins after high-performance gel filtration chromatography. *J Lipid Res.* 1991;32:859–866.
- Skalen K, Gustafsson M, Rydberg EK, Hulten LM, Wiklund O, Innerarity TL, Boren J. Subendothelial retention of atherogenic lipoproteins in early atherosclerosis. *Nature.* 2002;417:750–754.
- Jeong T, Schissel SL, Tabas I, Pownall HJ, Tall AR, Jiang X. Increased sphingomyelin content of plasma lipoproteins in apolipoprotein E knockout mice reflects combined production and catabolic defects and enhances reactivity with mammalian sphingomyelinase. *J Clin Invest.* 1998;101:905–912.
- Williams KJ, Tabas I. The response-to-retention hypothesis of early atherogenesis. *Arterioscler Thromb Vasc Biol.* 1995;15:551–561.
- Puri V, Jefferson JR, Singh RD, Wheatley CL, Marks DL, Pagano RE. Sphingolipid storage induces accumulation of intracellular cholesterol by stimulating SREBP-1 cleavage. *J Biol Chem.* 2003;278:20961–20970.
- Worgall TS, Juliano RA, Seo T, Deckelbaum RJ. Ceramide synthesis correlates with the posttranscriptional regulation of the sterol-regulatory element-binding protein. *Arterioscler Thromb Vasc Biol.* 2004;24:943–948.
- Leventhal AR, Chen W, Tall AR, Tabas I. Acid sphingomyelinase-deficient macrophages have defective cholesterol trafficking and efflux. *J Biol Chem.* 2001;276:44976–44983.
- Plump AS, Smith JD, Hayek T, Aalto-Setälä K, Walsh A, Verstuyft JG, Rubin EM, Breslow JL. Severe hypercholesterolemia and atherosclerosis in apolipoprotein E-deficient mice created by homologous recombination in ES cells. *Cell.* 1992;71:343–353.
- Mandala S, Hajdu R, Bergstrom J, Quackenbush E, Xie J, Milligan J, Thornton R, Shei GJ, Card D, Keohane C, Rosenbach M, Hale J, Lynch CL, Rupprecht K, Parsons W, Rosen H. Alteration of lymphocyte trafficking by sphingosine-1-phosphate receptor agonists. *Science.* 2002;296:346–349.
- Siess W. Athero- and thrombogenic actions of lysophosphatidic acid and sphingosine-1-phosphate. *Biochim Biophys Acta.* 2002;1582:204–215.
- Lee H, Liao JJ, Graeler M, Huang MC, Goetzl EJ. Lysophospholipid regulation of mononuclear phagocytes. *Biochim Biophys Acta.* 2002;1582:175–177.
- Cheng J, Park TS, Fischl AS, Ye XS. Cell cycle progression and cell polarity require sphingolipid biosynthesis in *Aspergillus nidulans*. *Mol Cell Biol.* 2001;21:6198–6209.
- Adachi-Yamada T, Gotoh T, Sugimura I, Tateno M, Nishida Y, Onuki T, Date H. De novo synthesis of sphingolipids is required for cell survival by down-regulating c-Jun N-terminal kinase in *Drosophila* imaginal discs. *Mol Cell Biol.* 1999;19:7276–7286.
- Dawkins JL, Hulme DJ, Brahmabhatt SB, Auer-Grumbach M, Nicholson GA. Mutations in SPTLC1, encoding serine palmitoyltransferase, long chain base subunit-1, cause hereditary sensory neuropathy type I. *Nat Genet.* 2001;27:309–312.
- Bejaoui K, Wu C, Scheffler MD, Haan G, Ashby P, Wu L, de Jong P, Brown RH Jr. SPTLC1 is mutated in hereditary sensory neuropathy, type 1. *Nat Genet.* 2001;27:261–262.